

Determination of rolling anisotropy by extensometry

A. SPOLIDOR

Ecole Nationale Supérieure des Mines de Saint Etienne, France

A theory is presented for the determination of three coefficients characterizing anisotropic materials. These new coefficients of anisotropy advantageously replace Lankford's classic empirical coefficient, r , in the definition of the anisotropy of a rolled sheet. It is shown how these coefficients ρ_0 , ρ_{45} and ρ_{90} may be deduced from the theory, provided certain assumptions are made concerning the rolled material. The validity of the theory was tested through experiments on rolled ultra high-purity iron sheet, ρ_0 , ρ_{45} and ρ_{90} being determined by means of a special purpose-built extensometer.

1. Introduction

The problem of determining the anisotropy of cold-rolled annealed metal using tensile tests on flat specimens cut from a rolled sheet has been the subject of studies for many years. The purpose of these studies was to define one specific characteristic of the sheet: its drawability.

In 1950, Lankford [1] proposed the coefficient, r , for which he is well known. It was defined as the ratio between the logarithms of the strains across the width and thickness of a flat tensile specimen stressed until it necks, i.e.

$$r = \frac{\log y_f/y_0}{\log x_f/x_0} \quad (1)$$

where x is the thickness of the specimen, y the width of the specimen, and 0 represents the initial state, and f the necked state.

Since its inception, this coefficient has always found great favour in industry, as determination is easy and the tensile test is simple to perform, at least in appearance. However, there is a fundamental objection to regarding the coefficient r as truly representative.

Firstly, it is arbitrary to choose only the initial and necked states for consideration. Lankford's hypothesis was that r remained constant throughout the test; however, experiment proves this is not the case. In fact, r varies with true stress, σ , as may be demonstrated by stopping the test and performing measurements at different stages of tensile extension (Fig. 1).

Secondly, this experimental difficulty may have a thermodynamic explanation. Because, in the plastic range, the tensile test is irreversible from the thermodynamic standpoint, the values obtained from this test depend not only on initial and final states but also on the path followed between these states, and this is not taken into account in the expression for r (the second Principle of Thermodynamics).

Inspection of Fig. 1 does indeed reveal that the plot of r versus σ may vary considerably; in particular, in any specific test, $dr/d\sigma$ changes each time the test is

interrupted. Thus the shapes of the r versus σ curves are not identical; this reveals the influence of the path followed.

Therefore, we can rewrite the expression for r in integral form

$$r = \frac{\int_{y_0}^{y_f} \frac{dy}{y}}{\int_{x_0}^{x_f} \frac{dx}{x}} \quad (2)$$

and focus our attention on the ratio of the differential components, thus

$$\rho = \left(\frac{dy}{y}\right) / \left(\frac{dx}{x}\right) = \left(\frac{dy}{dx}\right) \left(\frac{x}{y}\right) \quad (3)$$

This defines a new instantaneous anisotropy coefficient which includes x , y , the derivative dy/dx and therefore the y versus x curve at each moment of the tensile test. Because this new coefficient takes into account the path followed by the metal during the tensile test process, it is legitimate to consider it representative of the metal's anisotropy, the objections to r no longer being valid for ρ . It should be pointed out that ρ versus σ plots have already been produced by SOLLAC and these revealed that ρ varied linearly with σ (Fig. 1).

It should be possible to apply this coefficient industrially on the basis of the experimental results obtained here for the anisotropy of annealed rolled ultra high-purity iron, starting from Hill's theory. The method has been applied here to calculate the anisotropy of annealed cold-rolled ultra high-purity iron. It should also be added in passing that the French SOLLAC and SOLMER companies have been directing their attention for some years to the advantages of using ρ to characterize the anisotropy of industrial rolled products [2].

2. Adaptation of Hill's theory

The coefficient, ρ , is introduced into the plastic theory of anisotropic materials by Hill's theory [3] as a

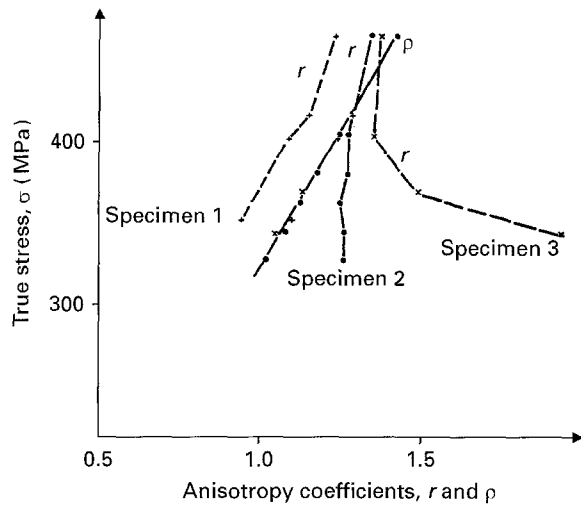


Figure 1 Plots of $r(\sigma)$ and $\rho(\sigma)$ where σ is the tensile stress. We see that r and ρ vary with σ . Moreover $r(\sigma)$ is not a simple function; on the other hand $\rho(\sigma)$ follows a straight line for the three tensile specimens studied (after SOLLAC experiments [2]).

parameter measuring anisotropy. This theory which is, in fact, based on the well-known three invariants $I_1 = \sigma_{ii}$, $I_2 = \sigma_{ij} \sigma_{kl}$, $I_3 = \sigma_{ij} \sigma_{kl} \sigma_{mm}$, of the stress tensor (σ_{ij}) , these three invariants being the coefficients (constants) of the third degree equation

$$\det.(\sigma_{ij}) - \sigma \delta_{ij} = 0 \quad (4)$$

[with $\delta_{ij} = 1 (i = j)$; $\delta_{ij} = 0 (i \neq j)$], σ_{ij} being the roots of this equation, as adapted and expanded in this paper, is proposed to account for the complex stresses and strains produced in such materials undergoing deformation. It calls on the state of stress of an "equivalent" material subjected to uniaxial tension so that the direction of the applied force has no effect on this state, the "equivalent" material thus being isotropic. The switch from the tensile properties (along the various directions) of the anisotropic material to the tensile properties of the equivalent material is performed using coefficients whose expressions are homogeneous with ρ .

2.1. Calculation of generalized stress, $\bar{\sigma}$, and of the corresponding strain $\bar{\epsilon}$

Let $F(\sigma_{ij})$ be a function of the internal stresses in the anisotropic material and $\bar{\sigma}$ the uniaxial tensile stress applied to the equivalent isotropic material. The calculation becomes a simple matter of determining $\bar{\sigma}$, assuming

$$F(\sigma_{ij}) - \bar{\sigma} = 0 \quad i = 1, 3 \quad (5)$$

$$j = 1, 3$$

$\bar{\sigma}$ is termed the uniaxial test "generalized" or "equivalent" stress related to the actual complex test imposed on the material. This complexity is due to the anisotropy of the actual material. The strain corresponding to $\bar{\sigma}$ is designated $\bar{\epsilon}$ (Fig. 2).

In an isotropic solid subjected to three principal stresses, σ_{11} , σ_{22} and σ_{33} are the solutions of the

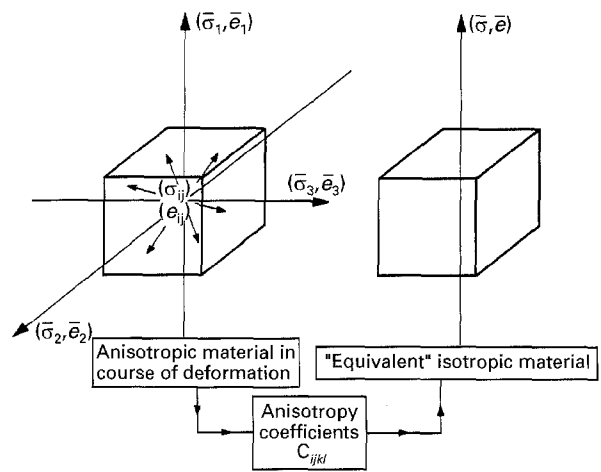


Figure 2 Hill's theory makes it possible to represent the complex stress state of a deformed anisotropic material in terms of the stress state of an "equivalent" isotropic material, and this can be determined by means of the coefficients of anisotropy.

equation

$$\det.(\sigma_{ij}) - \sigma \delta_{ij} = \sigma^3 - I_1 \sigma^2 - I_2 \sigma - I_3 = 0 \quad (6)$$

where

$$I_1 = \sigma_{11} + \sigma_{22} + \sigma_{33} \quad (7a)$$

$$I_2 = -(\sigma_{11}\sigma_{22} + \sigma_{22}\sigma_{33} + \sigma_{11}\sigma_{33}) + \sigma_{12}^2 + \sigma_{13}^2 + \sigma_{23}^2 \quad (7b)$$

$$I_3 = -\sigma_{11}\sigma_{23}^2 - \sigma_{22}\sigma_{13}^2 - \sigma_{33}\sigma_{12}^2 + 2\sigma_{12}\sigma_{23}\sigma_{31} + \sigma_{11}\sigma_{22}\sigma_{33} \quad (7c)$$

are the coefficients (constants) of this equation. Therefore, I_1 , I_2 and I_3 are stress tensor invariants in a rotation of the reference axes used to measure σ_{11} , σ_{22} and σ_{33} . In this isotropic material, $\bar{\sigma}$, which remains invariant whatever direction is chosen, will therefore be a function of I_1 , I_2 , I_3 , and we can write

$$\bar{\sigma} = f(I_1, I_2, I_3) \quad (8)$$

If we assume that hydrostatic pressure has no influence on deformation and that F is an even function of σ'_{ij} in the deviatoric tensor, we are led to the expression

$$\bar{\sigma} = F(I_2) \quad (9)$$

where I_2 is the quadratic invariant expression in the deviatoric tensor.

Similarly, for the anisotropic material, we shall assume that

$$\bar{\sigma} = F(J_2) = J_2^{1/2} \quad (10)$$

in the deviatoric tensor, where F has the dimensions of stress and the terms composing this new invariant J_2 are multiplied by coefficients of anisotropy C

$$J_2 = \frac{\sum_{ijkl} C_{ijkl} \sigma_{ij} \sigma_{kl}}{\sum_{ijkl} C_{ijkl}} \quad (11)$$

giving J_2 the form of a weighted mean (see Appendix).

Setting

$$H = \sum_{ijkl} C_{ijkl} \quad (12)$$

we can write

$$J_2 = \frac{1}{H} \sum_{ijkl} C_{ijkl} \sigma_{ij} \sigma_{kl} \quad (13)$$

Furthermore, energy conservation during the deformation can be written

$$\begin{aligned} dW &= \sum_{ij} \sigma_{ij} de_{ij} \\ &= \bar{\sigma} d\bar{\epsilon} \end{aligned} \quad (14)$$

where de_{ij} is the true strain increment in the ij direction and $d\bar{\epsilon}$ is the "generalized" strain associated with $\bar{\sigma}$. This energy-conservation relationship defines $d\bar{\epsilon}$.

2.2. Calculation of anisotropy coefficients

C_{ijkl}

From the mathematical homogeneity of F , we deduce

$$\bar{\sigma} = F(\sigma_{ij}) \quad (15)$$

or

$$\begin{aligned} \sum_{ij} \sigma_{ij} \frac{\partial F}{\partial \sigma_{ij}} &= F \\ &= \bar{\sigma} \end{aligned} \quad (16)$$

which leads to

$$\begin{aligned} dW &= \sum_{ij} \sigma_{ij} de_{ij} = \bar{\sigma} d\bar{\epsilon} = \\ &= d\bar{\epsilon} \sum_{ij} \sigma_{ij} \frac{\partial F}{\partial \sigma_{ij}} \end{aligned} \quad (17)$$

from Equation 16. Therefore

$$\sum_{ij} \sigma_{ij} de_{ij} = \sum_{ij} \sigma_{ij} \left(d\bar{\epsilon} \frac{\partial F}{\partial \sigma_{ij}} \right) \quad (18)$$

so

$$de_{ij} = d\bar{\epsilon} \frac{\partial F}{\partial \sigma_{ij}} \quad (19)$$

which is the normality condition: the strain vector de_{ij} is orthogonal to the yield surface $F(\sigma_{ij}) = k^2$.

From the expression

$$\begin{aligned} \bar{\sigma} &= F(J_2) \\ &= J_2^{1/2} \end{aligned} \quad (20)$$

and from Equations 13 and 19, we can write

$$de_{ij} = \frac{d\bar{\epsilon}}{H\bar{\sigma}} \sum_{ijkl} C_{ijkl} \sigma_{kl} \quad (21)$$

– We can now write the expression for the work increment

$$dW = \sum_{ij} \sigma_{ij} de_{ij} \quad (22)$$

and this, by application of Equation 21, becomes

$$dW = \sum_{ij} \sigma_{ij} \left(\frac{d\bar{\epsilon}}{H\bar{\sigma}} \sum_{ijkl} C_{ijkl} \sigma_{kl} \right) \quad (23)$$

$$dW = \frac{d\bar{\epsilon}}{H\bar{\sigma}} \sum_{ijkl} C_{ijkl} \sigma_{ij} \sigma_{kl} \quad (24)$$

which is a scalar function with dummy indices i, j, k and l .

We can therefore operate on these indices without changing the value of dW . Thus

$$\begin{aligned} dW &= \frac{d\bar{\epsilon}}{H\bar{\sigma}} C_{ijkl} \sigma_{ij} \sigma_{kl} \\ &= \frac{d\bar{\epsilon}}{H\bar{\sigma}} \sum_{ijkl} C_{klij} \sigma_{kl} \sigma_{ij} \end{aligned} \quad (25)$$

and we deduce that $C_{ijkl} = C_{klij}$.

– Let us assume that there is a single principal stress, σ_{ii} ; we may write that it produces a principal strain, de_{ii}

$$de_{ii} = \frac{d\bar{\epsilon}}{H\bar{\sigma}} C_{iiii} \sigma_{ii} \neq 0 \quad (26)$$

so $C_{iiii} \neq 0$.

σ_{ii} may also produce a strain de_{jj} (by conservation of volume within the plastic range)

$$de_{jj} = \frac{d\bar{\epsilon}}{H\bar{\sigma}} C_{jjii} \sigma_{ii} \neq 0 \quad (27)$$

We therefore conclude that $C_{jjii} = C_{iijj} \neq 0$.

– Let us assume that there is a single shear stress, σ_{ij} ; we may write that it produces a shear strain

$$de_{ij} = \frac{d\bar{\epsilon}}{H\bar{\sigma}} C_{ijij} \sigma_{ij} \neq 0 \quad (28)$$

so $C_{ijij} \neq 0$, and since $\sigma_{ij} = \sigma_{ji}$, $C_{ijij} = C_{jiji} \neq 0$.

On the other hand, σ_{ij} cannot produce a principal strain de_{kk} so $de_{kk} = 0$ and, from Equation 21

$$de_{kk} = \frac{d\bar{\epsilon}}{H\bar{\sigma}} C_{kkij} \sigma_{ij} = 0 \quad (29)$$

therefore $C_{kkij} = C_{ijkk} = 0$.

– Finally we come to the non-zero anisotropy coefficients

$$\begin{aligned} C_{iiij} \neq 0 \quad i = 1, 3; j = 1, 3 \\ \text{principal stress system} \end{aligned} \quad (30a)$$

$$C_{ijij} \neq 0 \quad i \neq j \quad \text{shear stress system} \quad (30b)$$

that is, nine non-zero coefficients

$$\begin{array}{ccc} C_{1111} & C_{2222} & C_{3333} \\ C_{1122} & C_{2233} & C_{1133} \\ C_{1212} & C_{2323} & C_{1313} \end{array}$$

out of the original 81 coefficients C_{ijkl} . Moreover, because the coefficients C_{iijj} ($i \neq j$) on the second

line are a linear combination of all C_{iiii} s, the relation being

$$C_{ijjj} = -\frac{1}{2}(C_{iiii} + C_{jjjj} - C_{kkkk}) \quad (31)$$

where $i \neq j \neq k$ and $i \neq k$, six independent coefficients remain [4-6]

$$C_{1111} \quad C_{2222} \quad C_{3333} \quad \text{principal stress system} \quad (32a)$$

$$C_{1212} \quad C_{2323} \quad C_{1313} \quad \text{shear stress system} \quad (32b)$$

The generalized stress $\bar{\sigma} = J_2^{1/2}$, where J_2 is defined by Equation 13, and may be written

$$\bar{\sigma} = \left\{ \frac{1}{H} \left[(\sigma_{11}\sigma_{22}\sigma_{33}) \mathcal{C}_n \begin{pmatrix} \sigma_{11} \\ \sigma_{22} \\ \sigma_{33} \end{pmatrix} + 2(\sigma_{12}\sigma_{23}\sigma_{31}) \mathcal{C}_c \begin{pmatrix} \sigma_{12} \\ \sigma_{23} \\ \sigma_{31} \end{pmatrix} \right] \right\}^{1/2} \quad (33)$$

where

$$\mathcal{C}_n = \begin{pmatrix} C_{1111} & C_{1122} & C_{1133} \\ C_{2211} & C_{2222} & C_{2233} \\ C_{3311} & C_{3322} & C_{3333} \end{pmatrix} \quad (34a)$$

and

$$\mathcal{C}_c = \begin{pmatrix} C_{1212} & 0 & 0 \\ 0 & C_{2323} & 0 \\ 0 & 0 & C_{1313} \end{pmatrix} \quad (34b)$$

The generalized strain is obtained by assuming conservation of energy, thus

$$\begin{aligned} dW &= \bar{\sigma} d\bar{e} \\ &= \sum_{ij} \sigma_{ij} de_{ij} \end{aligned} \quad (35)$$

and

$$\begin{aligned} d\bar{e} &= \left\{ H \left[(de_{11}de_{22}de_{33}) \mathcal{C}_n^{-1} \begin{pmatrix} de_{11} \\ de_{22} \\ de_{33} \end{pmatrix} + 2(de_{12}de_{23}de_{31}) \mathcal{C}_c^{-1} \begin{pmatrix} de_{12} \\ de_{23} \\ de_{31} \end{pmatrix} \right] \right\}^{1/2} \end{aligned} \quad (36)$$

2.3. Calculation of instantaneous coefficient of anisotropy, ρ

From Equation 19, $de_{ij} = d\bar{e}(d\bar{\sigma}/d\sigma_{ij})$ and from Equation 33

$$\begin{pmatrix} de_{11} \\ de_{22} \\ de_{33} \end{pmatrix} = \frac{d\bar{e}}{H\bar{\sigma}} \mathcal{C}_n \begin{pmatrix} \sigma_{11} \\ \sigma_{22} \\ \sigma_{33} \end{pmatrix} \quad (37a)$$

$$\begin{pmatrix} de_{12} \\ de_{23} \\ de_{31} \end{pmatrix} = \frac{d\bar{e}}{H\bar{\sigma}} \mathcal{C}_c \begin{pmatrix} \sigma_{12} \\ \sigma_{13} \\ \sigma_{31} \end{pmatrix} \quad (37b)$$

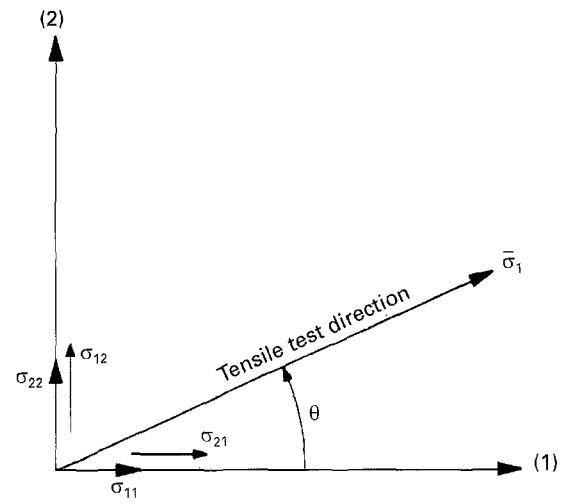


Figure 3 Diagram showing change of axes; (1) the rolling direction; (2) the transverse direction.

Let us assume a uniaxial tensile test with the tensile axis inclined at an angle θ to the principal axis of anisotropy (Fig. 3).

The stress tensor measured in a reference system based on the tensile specimen axis is worked out from the tensor measured along the principal axis of anisotropy by applying a rotation matrix, R

$$R = \begin{pmatrix} \cos^2\theta & \sin^2\theta & 2\sin\theta\cos\theta \\ \sin^2\theta & \cos^2\theta & -2\sin\theta\cos\theta \\ -\sin\theta\cos\theta & \sin\theta\cos\theta & \cos^2\theta - \sin^2\theta \end{pmatrix} \quad (38)$$

giving

$$\begin{pmatrix} \bar{\sigma}_1 \\ \bar{\sigma}_2 \\ \bar{\sigma}_{12} \end{pmatrix} = R \begin{pmatrix} \sigma_{11} \\ \sigma_{22} \\ \sigma_{12} \end{pmatrix} \quad (39)$$

Because, for a uniaxial tensile test, we may write $\bar{\sigma}_2 = 0, \bar{\sigma}_{12} = 0$, we obtain

$$\begin{pmatrix} \sigma_{11} \\ \sigma_{22} \\ \sigma_{12} \end{pmatrix} = R^{-1} \begin{pmatrix} \bar{\sigma}_1 \\ 0 \\ 0 \end{pmatrix} \quad (40)$$

Similarly

$$\begin{pmatrix} d\bar{e}_1 \\ d\bar{e}_2 \\ d\bar{e}_{12} \end{pmatrix} = R \begin{pmatrix} de_{11} \\ de_{22} \\ de_{12} \end{pmatrix} \quad (41)$$

where de_1 is the true deformation along the tensile specimen axis. Taking Equation 37a and b we can then write

$$\begin{pmatrix} d\bar{e}_1 \\ d\bar{e}_2 \\ d\bar{e}_{12} \end{pmatrix} = R \frac{d\bar{e}}{H\bar{\sigma}} \underbrace{\begin{pmatrix} C_{1111} & C_{1122} & 0 \\ C_{2211} & C_{2222} & 0 \\ 0 & 0 & C_{1212} \end{pmatrix}}_{\text{matrix } A} \begin{pmatrix} \sigma_{11} \\ \sigma_{22} \\ \sigma_{12} \end{pmatrix} \quad (42)$$

Because only planar anisotropy is involved, we assume

$$de_{13} = de_{23} = 0 \quad (43)$$

and consequently

$$C_{1313} = C_{2323} = 0 \quad (44)$$

and, by virtue of Equation 40

$$\begin{pmatrix} d\bar{e}_1 \\ d\bar{e}_2 \\ d\bar{e}_{12} \end{pmatrix} = \frac{d\bar{e}}{H\bar{\sigma}} RAR^{-1} \begin{pmatrix} \bar{\sigma}_1 \\ 0 \\ 0 \end{pmatrix} \quad (45)$$

where A is the matrix of the C_{ijkl} coefficients [in Equation 42].

Furthermore, from Equation 37a and b and taking the planar anisotropy into account, $\bar{\sigma}_3 = \sigma_{33} = 0$, we obtain

$$d\bar{e}_3 = de_{33} = \frac{d\bar{e}}{H\bar{\sigma}} (C_{3311} C_{3322}) \begin{pmatrix} \bar{\sigma}_1 \\ \bar{\sigma}_{22} \end{pmatrix} \quad (46)$$

and from Equation 40 this equals

$$d\bar{e}_3 = \frac{d\bar{e}}{H\bar{\sigma}} (C_{3311} \cos^2 \theta + C_{3322} \sin^2 \theta) \bar{\sigma}_1 \quad (47)$$

We can then calculate the ratios $d\bar{e}_1/d\bar{e}_3$, $d\bar{e}_2/d\bar{e}_3$, $d\bar{e}_{12}/d\bar{e}_3$ which have the same form as the instantaneous anisotropy coefficient given in Equation 3. Thus

$$\begin{pmatrix} d\bar{e}_1/d\bar{e}_3 \\ d\bar{e}_2/d\bar{e}_3 \\ d\bar{e}_{12}/d\bar{e}_3 \end{pmatrix} = \frac{RAR^{-1}}{C_{3311} \cos^2 \theta + C_{3322} \sin^2 \theta} \begin{pmatrix} 1 \\ 0 \\ 0 \end{pmatrix} \quad (48)$$

In fact, in Equation (3) we dealt with deformations along the width and thickness of the test specimen; we shall therefore pay particular attention to the ratio $d\bar{e}_2/d\bar{e}_3$ with $d\bar{e}_2 = dy/y$ and $d\bar{e}_3 = dx/x$.

If it is assumed that the tensile tests are performed at 0° , 45° and 90° to the rolling axis, we obtain the following relationships, by application of Equation 48

$$\rho_0 = \left(\frac{d\bar{e}_2}{d\bar{e}_3} \right)_{\theta=0^\circ} = \frac{C_{1111} + C_{2222} - C_{3333}}{C_{1111} - C_{2222} + C_{3333}} \quad (49a)$$

$$\rho_{45} = \left(\frac{d\bar{e}_2}{d\bar{e}_3} \right)_{\theta=45^\circ} = -\frac{1}{2} + \frac{C_{1212}}{C_{3333}} \quad (49b)$$

$$\rho_{90} = \left(\frac{d\bar{e}_2}{d\bar{e}_3} \right)_{\theta=90^\circ} = \frac{C_{1111} + C_{2222} - C_{3333}}{-C_{1111} + C_{2222} + C_{3333}} \quad (49c)$$

Taking Equations 40 and 49a-c and also the following equation

$$H = \sum_{ijkl} C_{ijkl} = 2C_{1212} \quad (50)$$

for planar anisotropy, Equation 33 for $\bar{\sigma}$ can be written as set out below

Equivalent tensile curve along the rolling direction
($\theta = 0^\circ$)

$$\bar{\sigma}_0 = \left[\frac{(\rho_0 + 1)\rho_{90}}{2(\rho_{45} + \frac{1}{2})(\rho_0 + \rho_{90})} \right]^{1/2} \bar{\sigma}_1 \quad (51)$$

$$= P_0 \bar{\sigma}_1$$

and applying Equation 36

$$d\bar{e}_0 = \frac{1}{P_0} d\bar{e}_1 \quad (52)$$

Equivalent tensile curve at 45° to the rolling direction
($\theta = 45^\circ$)

$$\bar{\sigma}_{45} = \left[\frac{\rho_{45} + 1}{2(2\rho_{45} + 1)} \right]^{1/2} \bar{\sigma}_1 = P_{45} \bar{\sigma}_1 \quad (53)$$

and applying Equation 36

$$d\bar{e}_{45} = \frac{1}{P_{45}} d\bar{e}_1 \quad (54)$$

As the doublet $(\bar{\sigma}_0, \bar{e}_0)$ must be an invariant versus the sampling in the rolled sheet and in accordance with the plasticity assumptions, it is sufficient to calculate two equivalent tensile curves ($\theta = 0^\circ$ and $\theta = 45^\circ$) to check their possible superposition on a graph, which will be done later in this paper.

We have thus developed a detailed calculation allowing us to connect the generalized or equivalent stress, $\bar{\sigma}$, in the isotropic material to the stress, $\bar{\sigma}_1$, effectively applied to the test specimen in the uniaxial tensile test. This has been achieved by using three instantaneous coefficients of anisotropy, ρ_0 , ρ_{45} and ρ_{90} , which have the form of Equation (3). The same is true for the generalized strain $d\bar{e}$.

ρ_0 , ρ_{45} and ρ_{90} may, therefore, be used to define the anisotropy of the rolled solid. These coefficients can be calculated from the results of tensile tests on specimens cut from the rolled sheet and oriented at 0° , 45° and 90° to the rolling direction, as will be seen in subsequent sections.

3. Application of theory to an anisotropic rolled sheet in the uniaxial tensile test. Determination of ρ coefficients of anisotropy

This theory only applies to a material that meets the following conditions

(i) There is no Bauschinger effect (F is an even function of σ_{ij}); there is continuity when changing from tension to compression;

(ii) hydrostatic pressure $\mathcal{H} = \frac{1}{3} \sum_i \sigma_{ii}$ has no effect on deformation. It follows that $\sum_i \sigma'_{ii} = 0$ in the deviatoric tensor;

(iii) the solid is practically incompressible: $\sum_i de_{ii} = 0$;

(iv) the solid has three orthogonal planes of symmetry for anisotropy; the normals to these planes being the principal axes of anisotropy;

(v) to a first approximation, we assume that the anisotropy coefficients are independent of stress during the tensile test, something that is not true in practice. Therefore we have to determine these coefficients at each stage in the deformation.

(vi) The deformation is independent of temperature and of strain rate during the test. In fact, the metal will be studied at different temperatures and strain rates and the values of these parameters which verify the other previous assumptions will be determined, if they exist.

Once we have set out these assumptions we can apply these theories and adapt our calculation to the case of an anisotropic rolled sheet material deformed in an uniaxial tensile test. This test is chosen because it is simple to put into practice.

Because the $\bar{\sigma}$ versus $\bar{\epsilon}$ curves are invariant when the reference axes of the rolled specimen are changed, we shall consider tensile tests along several directions in this rolled sheet. In particular, we shall consider tensile tests performed along the rolling direction and at 45° to this direction. The calculation outlined in Section 2 resulted in Equations 51–54 and these enable curves of $\bar{\sigma}$ versus $\bar{\epsilon}$ to be plotted for tensile tests at 0° and 45° to the rolling direction.

In these equations, $\bar{\sigma}_1$ and $d\bar{\epsilon}_1$ are the true stress and the differential of the strain actually applied to the specimen. The new coefficients, ρ_0 , ρ_{45} and ρ_{90} , which are functions of the six independent coefficients C_{ijkl} , appear in these equations. ρ_0 , ρ_{45} and ρ_{90} are defined as the ratios of the true strains across the width and thickness of flat specimens taken at 0°, 45° and 90° to the rolling direction.

$$\rho_0 = \left(\frac{d\bar{\epsilon}_2}{d\bar{\epsilon}_3} \right)_{\theta=0^\circ} \quad (55a)$$

$$\rho_{45} = \left(\frac{d\bar{\epsilon}_2}{d\bar{\epsilon}_3} \right)_{\theta=45^\circ} \quad (55b)$$

$$\rho_{90} = \left(\frac{d\bar{\epsilon}_2}{d\bar{\epsilon}_3} \right)_{\theta=90^\circ} \quad (55c)$$

These new anisotropy coefficients have the same form as those in Equation 3. The only difference is that our calculation means that three coefficients are required to describe the anisotropy of a rolled sheet. These three coefficients can be calculated if the metal under study satisfies the assumptions set out in this section. The “equivalent” material whose deformation is governed by $\bar{\sigma}$ and $\bar{\epsilon}$ must, therefore, be isotropic; and for tests performed at 0° and 45° to the rolling direction, the curves $\bar{\sigma}_0 = \phi_0(\bar{\epsilon}_0)$ and $\bar{\sigma}_{45} = \phi_{45}(\bar{\epsilon}_{45})$, given by Equations 51–54 should coincide. Provided this condition is met, the coefficients ρ_0 , ρ_{45} and ρ_{90} may be adopted to characterize rolled sheet anisotropy.

4. Description of the extensometer adapted to verify this theory in the case of planar anisotropy (rolled sheet)

Because the coefficients ρ_0 , ρ_{45} and ρ_{90} have the form $(dy/dx)(x/y)$ (Equation 3), it is necessary to find the derivative dy/dx and therefore the curve y versus x of the width of the tensile test specimen plotted against its thickness over time.

It was possible to establish this curve by designing and constructing an extensometer using an inductive sensor and allowing the width and thickness of the specimen to be recorded simultaneously on a two-channel chart recorder (Fig. 4a–c). When the test was set up, the weight of the extensometer was balanced by two counterweights (Fig. 4d).

Tests were performed at different speeds of testing and at three temperatures: ambient, 300 °C achieved by passing a heavy current through the specimen (Joule effect), and –40 °C achieved by cooling the specimen using liquid nitrogen and conducting heat away through two rods of pure copper. The temperature was measured by a thermocouple clamped to the specimen.

The following testing speeds, V , were chosen: 0.02, 0.2, 2 and 20 cm min⁻¹ at ambient temperature. For temperatures of –40 and 300 °C, tests were made only at 20 cm min⁻¹ so that the specimen remained under isothermal conditions.

Finally, the accuracy achieved was on the order of 10 μm for the width y and 5 μm for the thickness x .

5. Calculation of coefficients of anisotropy for a rolled high-purity iron sheet

The above calculations were applied to determine the coefficients of anisotropy of a flat-rolled ultra high-purity iron. The flat test pieces considered were realized on the basis of the following sequences:

- (i) ultra high-purity iron, obtained by chemical extraction with butyl acetate and FeCl₃ sublimation, pure iron sponge fabrication from oxide hydrogen reduction, zone refining of the sponge under vacuum and refusion in an ingot by an electron beam;
- (ii) purity – all elements under 1 p.p.m.;
- (iii) flat forging and hot rolling of the ingot at ~1100 °C;
- (iv) cleaning of the hot-rolled sheet by grinding;
- (v) cold rolling to 1 mm thick (90% reduction).

The crystallographic anisotropy of such a cold-rolled sheet, before annealing, is given on the {110} pole figure established by the author on an X-ray goniometer by complementary reflection and transmission techniques [7] Figs 1a and 13b, [8], [9], Figs 1a and 9b). Test specimens having the dimensions shown in Fig. 5 were cut at 0°, 45° and 90° to the rolling direction (Fig. 6). These specimens were then annealed at 700 °C in a secondary vacuum and set up, on a tensile test machine fitted with the extensometer described in Section 4.

As this theory does not take temperature T , and strain rate, $\dot{\epsilon} = d\bar{\epsilon}_1/dt$, in the tensile test into account, we carried out our tests at the temperatures and with the testing speeds listed earlier.

Test data were recorded and processed in the following stages:

- (i) initial specimen cross-sectional dimensions x_0 and y_0 were measured;
- (ii) the variations of \mathcal{F} with y and of x with y were recorded graphically, \mathcal{F} being the force applied and y the abscissa. This was done for each temperature T and for each speed, V , which were all recorded for each of the three angles of 0°, 45° and 90° to the rolling direction. Thus, for each preset pair of parameters (T, V) , three \mathcal{F} versus y and x versus y curves are required for any specific planar anisotropy calculation (Fig. 7a–c);
- (iii) the curve of $\bar{\sigma}_1 = \mathcal{F}/S = \mathcal{F}/xy$ versus y was plotted;

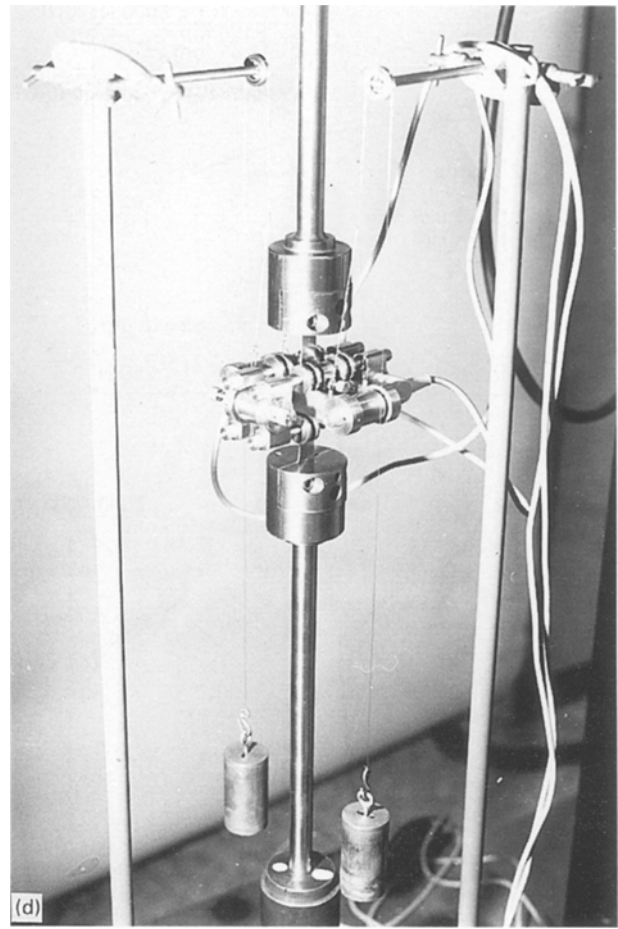
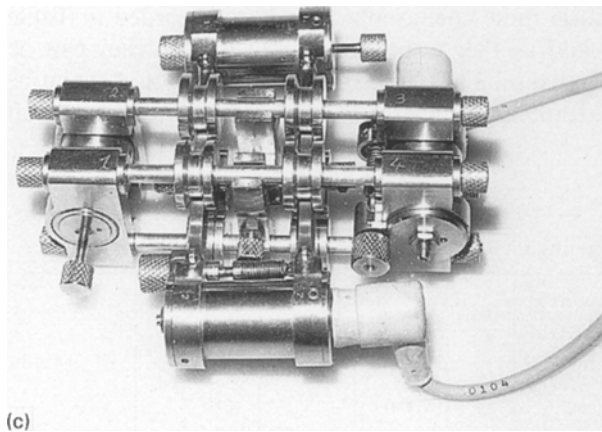
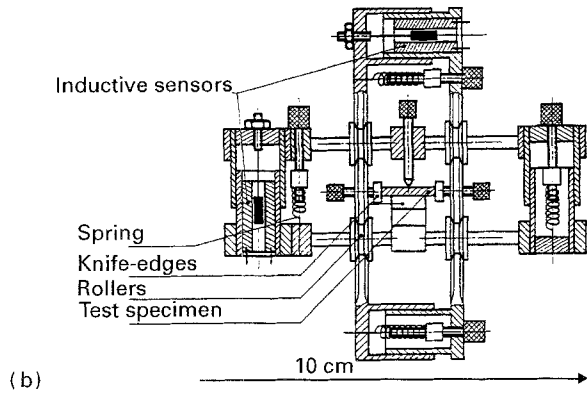
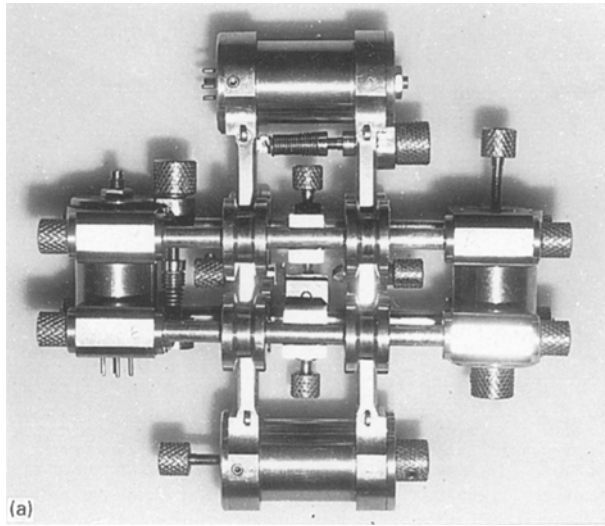


Figure 4 The extensometer: (a) top view, (b) schematic diagram. This extensometer was especially designed and built for this study using non-magnetic austenitic stainless steel. (c) The extensometer with its electronic connectors. (d) The extensometer set up on the tensile testing machine.

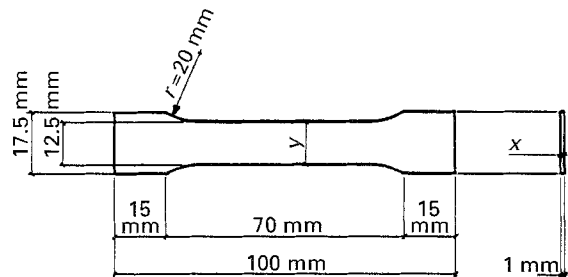


Figure 5 The flat tensile test bar based on ISO 12.5 mm × 50 mm specimen.

(iv) a table was drawn up with the main horizontal divisions corresponding to different values of $\bar{\sigma}_1$ (Table I). In this table, $\bar{\sigma}$ and $\bar{\epsilon}$ are calculated from Equation 51–54; $\bar{\epsilon}$ is calculated by graphic integration of the function

$$\bar{\epsilon} = \int_{\bar{\epsilon}_{1\text{initial}}}^{\bar{\epsilon}_1} Q(u) du$$

where

$$Q(\bar{\epsilon}_1) = \frac{1}{P}$$

which therefore requires the graph of Q versus $\bar{\epsilon}_1$ to be plotted (Fig. 8).

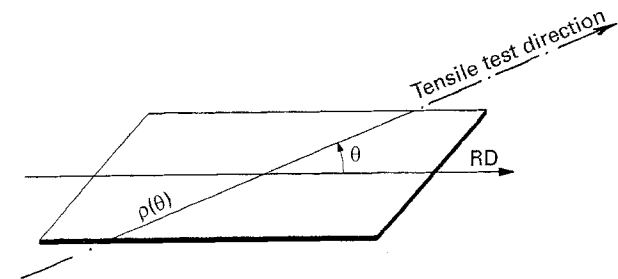


Figure 6 Cutting the tensile specimen from sheet: definition of θ (RD is the rolling direction). The new instantaneous anisotropy coefficient, ρ , is a function of θ .

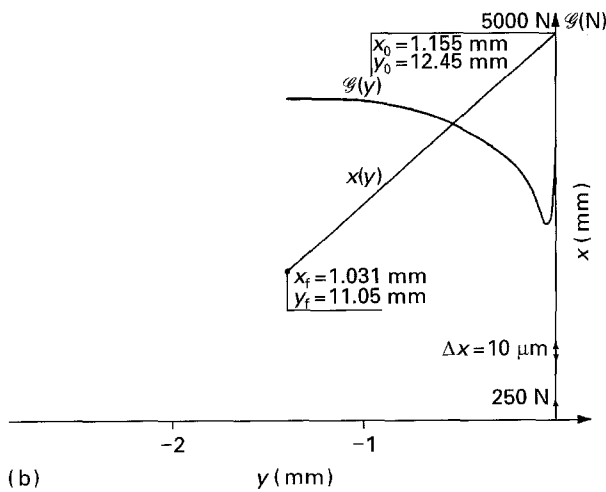
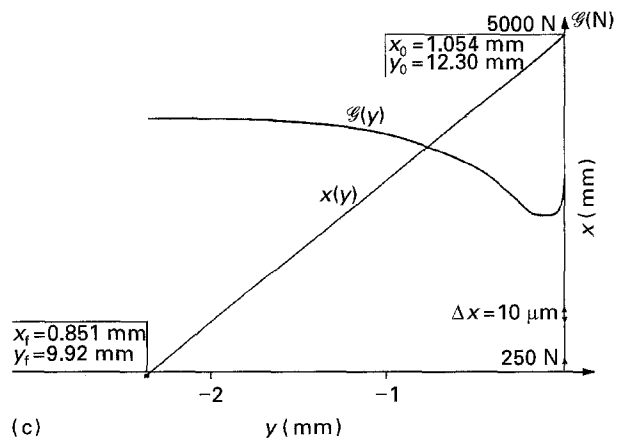
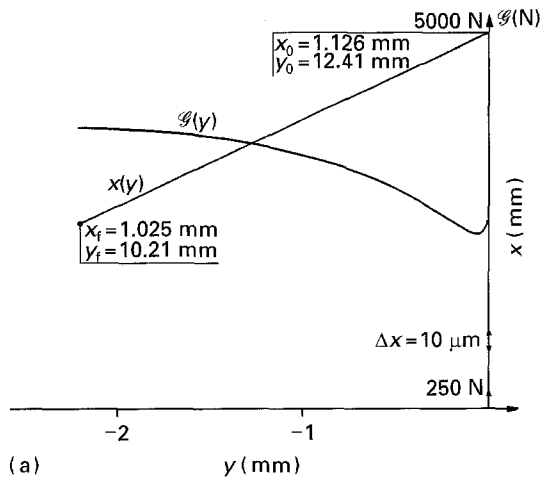


Figure 7a $G(y)$ and $x(y)$ plots obtained by extensometer measurements on tensile tests on specimens taken (a) along the rolling direction, $\theta = 0^\circ$; (b) at 45° to the rolling direction, $\theta = 45^\circ$ and (c) at 90° to the rolling direction, $\theta = 90^\circ$; $T = 20^\circ$, $V = 2 \text{ cm min}^{-1}$ in all cases.

far considered, i.e. for $T = 20^\circ \text{C}$ and $V = 2 \text{ cm min}^{-1}$, the ϕ_0 and ϕ_{45} curves virtually coincide (Fig. 9). This coincidence of the two curves is not observed for any of the other temperatures or testing speeds (Fig. 10a-c).

It may therefore be concluded, on the basis of our statements in Section 3, that for tensile testing at $T = 20^\circ \text{C}$ and $V = 2 \text{ cm min}^{-1}$ the ultra high-purity iron investigated conforms with previous hypothesis. Our theory applies in this case and we can determine the value of the coefficients ρ_0 , ρ_{45} and ρ_{90} which characterize the anisotropy of the rolled sheet. Because these coefficients have been recorded in Table I and as they appear to vary with $\bar{\sigma}_1$, they can be plotted on a graph against this stress (Fig. 11) and be extrapolated linearly to zero stress (initial material

To sum up, Table I gives values of $\bar{\sigma}_0$ for \bar{e}_0 and $\bar{\sigma}_{45}$ for \bar{e}_{45} and therefore gives functions ϕ_0 and ϕ_{45} , the curves of which may be plotted on the same graph. It can be seen that in the case so

TABLE I Calculation of $\bar{\sigma} = \phi_0(\bar{e})$ for $\theta = 0^\circ$ and $\theta = 45^\circ$ (ultra high-purity iron) $T = 20^\circ \text{C}$, $V = 2 \text{ cm min}^{-1}$

θ (deg)	x_0 (mm)	y_0 (mm)	$\bar{\sigma}_1$ (MPa) $= \frac{G}{xy}$ (N)	x (mm)	y (mm)	$\frac{dy}{dx}$	$\rho = \frac{dyx}{dx y}$	P	$\bar{\sigma} =$ $P \cdot \bar{\sigma}_1$ (MPa)	$Q(\bar{e}_1)$ $= 1/P$	\bar{e}_1 $= \log \frac{x_0 y_0}{xy}$ $\times 10^{-4}$	$\bar{e} =$ $\int_{\bar{e}_{\text{initial}}}^{\bar{e}_1} Q(u) du$ $\times 10^{-4}$	
0°	1.126	12.41		3051	1.109	11.85	21.21	1.985	0.625	145.12	1.6	613	0
45°	1.155	12.45	232.2	3280	1.153	12.25	9.5	0.894	0.583	135.37	1.715	179	0
90°	1.054	12.30		2815	1.017	11.92	13.41	1.144					
0°	1.126	12.41		3357	1.090	11.48	21.21	2.014	0.627	168.22	1.595	1103	782
45°	1.155	12.45	268.3	3660	1.132	12.05	9.5	0.892	0.583	156.4	1.715	527	597
90°	1.054	12.30		3142	1.001	11.70	13.41	1.147					
0°	1.126	12.41		3526	1.074	11.14	21.74	2.096	0.620	182.7	1.613	1552	1502
45°	1.155	12.45	294.7	3880	1.111	11.85	9.5	0.890	0.583	171.8	1.715	882	1206
90°	1.054	12.30		3342	0.987	11.49	12.86	1.105					
0°	1.126	12.41		3703	1.038	10.51	19.25	1.901	0.604	205.0	1.656	2475	3000
45°	1.155	12.45	339.4	4100	1.055	11.45	9.5	0.875	0.583	197.87	1.712	1742	2580
90°	1.054	12.30		3587	0.953	11.09	11.76	1.010					
0°	1.126	12.41		3700	1.025	10.21	47.6	4.778	0.593	209.62	1.686	2891	3694
45°	1.155	12.45	353.5	3921	1.044	10.625	9.5	0.933	0.581	205.38	1.721	2595	4145
90°	1.054	12.30		3635	0.940	10.94	11.76	1.010					

$$\bar{\sigma} = \Phi_0(\bar{e})$$

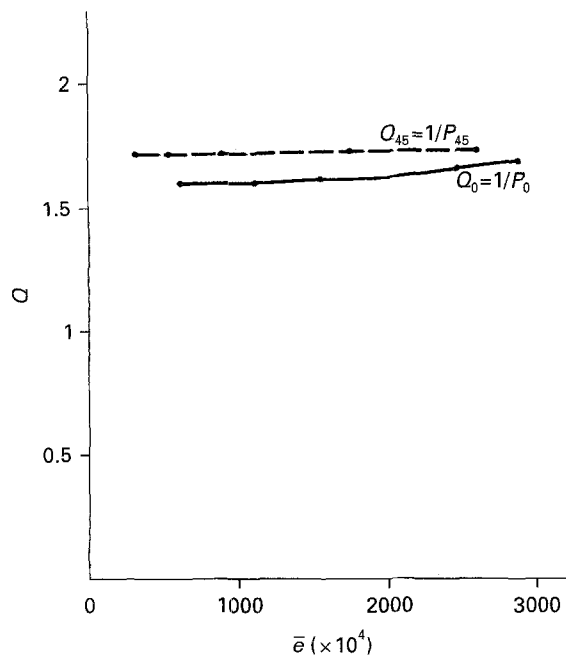


Figure 8 $Q_0(\bar{e}_0^0)$ and $Q_{45}(\bar{e}_{45}^{45})$ plots from which \bar{e}_0 and \bar{e}_{45} can be calculated by graphic integration. $T = 20^\circ\text{C}$, $V = 2 \text{ cm min}^{-1}$.

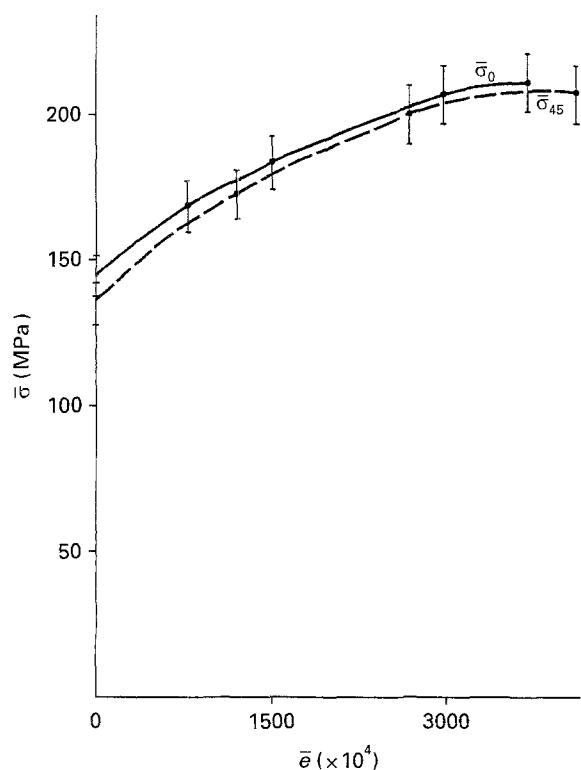
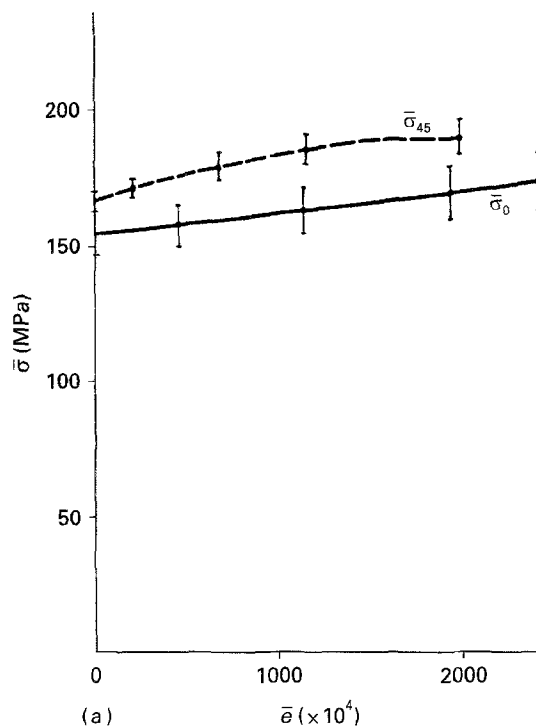


Figure 9 Plot of graphs of $\bar{\sigma}_0 = \phi_0(\bar{e}_0)$ and $\bar{\sigma}_{45} = \phi_{45}(\bar{e}_{45})$ for tensile tests at $T = 20^\circ\text{C}$ and $V = 2 \text{ cm min}^{-1}$. It can be seen that the curves virtually coincide in this case.

condition), for example by using the method of least squares. It should be noted that the points representing ρ_{45} and ρ_{90} fall practically on a straight line when plotted against $\bar{\sigma}_1$, a fact that was observed by SOLLAC [2] in similar tensile tests (Fig. 1).

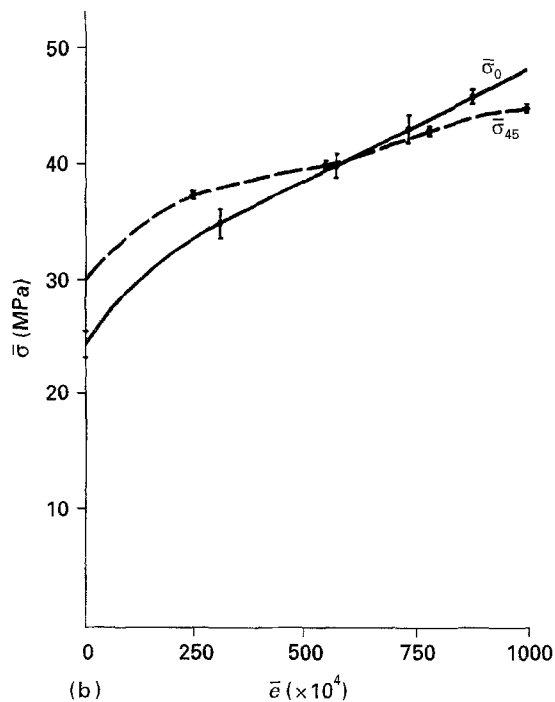
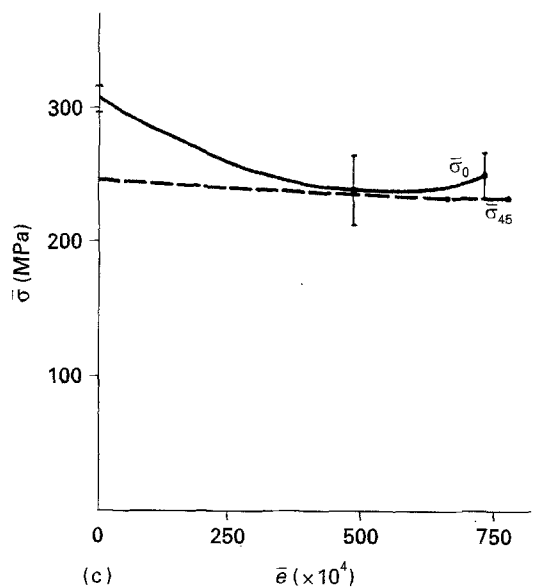


Figure 10 Unlike the test in Fig. 9, the ϕ_0 and ϕ_{45} curves do not coincide. This may be caused by the fact that our assumptions are not satisfied by the material for these tensile test parameters. (a) $T = 20^\circ\text{C}$, (b) $T = 300^\circ\text{C}$, (c) $T = -40^\circ\text{C}$, $V = 20 \text{ cm min}^{-1}$ in all cases.



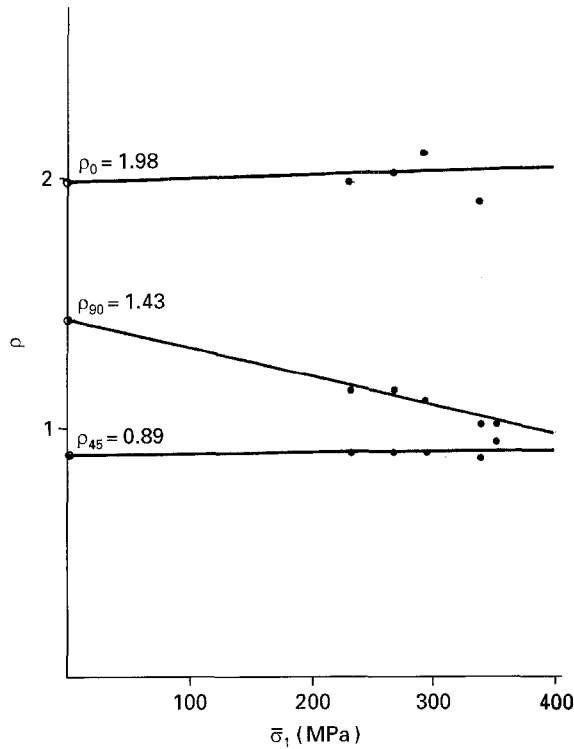


Figure 11 Variation of ρ_0 , ρ_{45} and ρ_{90} with $\bar{\sigma}_1$ applied to the test specimens. Extrapolation to the initial state ($\bar{\sigma}_1 = 0$) provides us with the coefficient of anisotropy values for the rolled material under study (ultra high-purity iron).

For the ultra high-purity iron under study, extrapolation to $\bar{\sigma}_1 = 0$ gives the following coefficients of anisotropy: $\rho_0 = 1.98$, $\rho_{45} = 0.89$, $\rho_{90} = 1.43$. These coefficients define the anisotropy of the material according to our study.

6. Conclusion

In place of Lankford's coefficient, r , we have introduced three new coefficients of anisotropy, ρ_0 , ρ_{45} and ρ_{90} . These are defined as the ratios between the true strains across the width and thickness of flat tensile test specimens taken at 0° , 45° and 90° to the rolling direction of the sheet investigated. Their relationship is given by Equation 3. These coefficients, in fact, proceed from our adaptation of Hill's theory to the calculation of the anisotropy of a flat-rolled sheet and they obey the 2nd Principle of Thermodynamics, on the contrary of r . They can be used to give a global description of the anisotropy of analogous products and notably of flat-rolled metal products used in industry.

We have achieved a practical application of these results in calculating the anisotropy of an annealed cold-rolled ultra high-purity iron sheet. Implementation consisted in using the uniaxial tensile test combined with an extensometer specially designed and constructed in our laboratory. We observed that the pure iron under investigation concurred with our hypothesis for tensile tests carried out at a temperature of 20°C and with a testing speed of 2 cm min^{-1} , values for which the ϕ_0 and ϕ_{45} curves coincided. These experimental results verify our theory and

calculations performed to apply it [7]. It should be noted that calculations which appear complicated have led us to simple results, essentially embodied in Equations 51–55. It is a simple matter to program these results into a computer so that the results of the various tensile tests can be processed and the ϕ_0 and ϕ_{45} curves plotted automatically. Applying this theory we managed to establish the following values for the three coefficients of anisotropy of the rolled, ultra high-purity iron sheet under study [7]: $\rho_0 = 1.98$; $\rho_{45} = 0.89$; $\rho_{90} = 1.43$.

It is then possible to describe and quantify a rolling texture on the basis of a fundamental plasticity theory, the formation of such rolling textures having been explained previously elsewhere [7–9].

Appendix. Demonstration of the validity of the expression for the J_2 .

We demonstrate below that the expression for J_2

$$J_2 = \frac{1}{H} \sum C_{ijkl} \sigma_{ij} \sigma_{kl} \quad (13)$$

which has the form of a weighted average, is legitimate.

The second invariant expression for an isotropic solid (limiting case) is as follows (in the deviatoric tensor)

$$I'_2 = \sigma_{12}^2 + \sigma_{13}^2 + \sigma_{23}^2 + \frac{1}{6} [(\sigma_{11} - \sigma_{22})^2 + (\sigma_{22} - \sigma_{33})^2 + (\sigma_{11} - \sigma_{33})^2] \quad (A1)$$

which can be written

$$I'_2 = \frac{1}{3} (\sigma_{11}^2 + \sigma_{22}^2 + \sigma_{33}^2) - \frac{1}{3} (\sigma_{11}\sigma_{22} + \sigma_{22}\sigma_{33} + \sigma_{11}\sigma_{33}) + \sigma_{12}^2 + \sigma_{23}^2 + \sigma_{13}^2 \quad (A2)$$

Moreover (from Equation 13)

$$J_2 = \frac{1}{H} [C_{iiii}\sigma_{ii}^2 + 2C_{ijjj}\sigma_{ii}\sigma_{jj} + 2C_{ijij}\sigma_{ij}^2] \quad (A3)$$

in accordance with the allowed expressions for C_{ijkl} (see Equations 31 and 32).

Consequently, at the limit for an isotropic material

$$\frac{C_{1111}}{H} = \frac{1}{3} \quad \text{with } C_{1111} = C_{2222} = C_{3333} \quad (A4)$$

$$\frac{2C_{1122}}{H} = -\frac{1}{3} \quad \text{with } C_{1122} = C_{1133} = C_{2233} \quad (A5)$$

$$2\frac{C_{1212}}{H} = 1 \quad \text{with } C_{1212} = C_{1313} = C_{2323} \quad (A6)$$

As $H = 2C_{1212}$ (see Equation 50), we have thus verified that Equation A6 always holds.

From Equations A4 and A5 we deduce that

$$C_{1111} = -2C_{1122} \quad (\text{A7})$$

which also holds (see Equation 31 with $C_{2222} = C_{3333}$).

In conclusion, the expression for J_2 is also valid for low anisotropies and at the limit for an isotropic solid.

References

1. W. T. LANKFORD, S. C. SNYDER and J. A. BAUSHER, *Trans. ASM* **42** (1950) 1197.
2. G. JEGADEN, J. VOINCHET and P. ROCQUET, *Mem. Sci. Rev. Metall.* **LIX** (4) (1962).
3. R. HILL, *The mathematical theory of plasticity* (Clarendon Press, Oxford, 1964).
4. M. J. HILLIER, *Mechanics of Sheet forming* (University of Waterloo, Mechanical Engineering Department, Waterloo, Ontario, 1968).
5. *Idem*, "Metallurgical plasticity" (Dept. de Métallurgie, Ecole Nationale Supérieure des Mines de Saint-Etienne, 1970).
6. R. N. DUBEY and M. J. HILLIER, *Basic Eng. ASME HQ* **71** (Met-p) March 1971.
7. A. SPOLIDOR, *These de Doctorat d'Etat és Sciences Physiques*, Université de Paris VI (1983).
8. A. SPOLIDOR, J. RIEU and C. GOUX, *J. Auto. Métall. Paris* (63) 3 October 1973.
9. A. SPOLIDOR and C. GOUX, *J. Mater. Sci.* **28** (1993) 4325.

*Received 2 February
and accepted 7 November 1995*